Resonant localized states and quantum percolation on random chains with power-law-diluted long-range couplings

2012 J. Phys.: Condens. Matter 24 205401

(http://iopscience.iop.org/0953-8984/24/20/205401)

J. Phys.: Condens. Matter **24** (2012) 205401 (6pp) doi:10.1088/0953-8984/24/20/205401

Resonant localized states and quantum percolation on random chains with power-law-diluted long-range couplings

S S de Albuquerque[1], F A B F de Moura[2] and M L Lyra[2]

[1] Curso de Física, Universidade Federal de Alagoas, Campus Arapiraca, Arapiraca-AL 57309-005, Brazil
[2] Instituto de Física, Universidade Federal de Alagoas, Maceió AL 57072-970, Brazil

Received 8 February 2012, in final form 15 March 2012
Published 18 April 2012
Online at stacks.iop.org/JPhysCM/24/205401

Abstract

We investigate the nature of one-electron eigenstates in power-law-diluted chains for which the probability of occurrence of a bond between sites separated by a distance r decays as $p(r) = p/r^{1+\sigma}$. Using an exact diagonalization scheme and a phenomenological finite-size scaling analysis, we determine the quantum percolation transition phase diagram in the full parameter space (p, σ). We show that the density of states displays singularities at some resonance energies associated with degenerate eigenstates localized in a pair of sites with special symmetries. This model is shown to present an intermediate phase for which there is classical percolation but no quantum percolation. Quantum percolation only takes place for $\sigma < 0.78$, a value larger than the corresponding one for the Anderson transition in long-ranged coupled chains with random diagonal disorder. The fractality of critical wavefunctions is also characterized.

1. Introduction

Anderson theory predicts the absence of extended one-electron eigenstates in low-dimensional ($d < 2$) systems with non-interacting electrons and uncorrelated disorder [1]. Therefore, the width of the time-dependent electronic wavepacket shall saturate in a finite region around the initial position after a long time evolution, especially in one-dimensional systems where the effects of disorder are more pronounced. In three-dimensional lattices, weak disorder promotes the localization of the high-energy eigenmodes [1–3]. It was demonstrated that two mobility edges appear separating localized states from extended states [4]. Recently, it has been shown that low-dimensional disordered systems can support extended states when special short-range [5–18] or long-range [8–18] correlations are present in the disorder distribution. From the experimental point of view, these theoretical predictions were useful to explain the transport properties of semiconductor superlattices [13] and the microwave transmission spectra of a single-mode waveguide with intentional correlated disorder [16].

Another ingredient that can promote the breakdown of Anderson localization in low-dimensional systems is the presence of long-range hoppings. In [19], it was shown that the dynamics of an electron in the one-dimensional Anderson model with non-random hoppings falling off as some power $(1/r^{\alpha})$ becomes faster for $1 < \alpha < 2$. For a low degree of disorder, the exponent $\alpha = 1.5$ indicates the onset for fast propagation, in agreement with the reported delocalization of states located close to one of the band edges [20–22]. Another interesting class of disordered system with long-range hoppings is the power-law random band matrix (PRBM) model [23–26]. This model describes one-dimensional electronic systems with random long-range hopping amplitudes with standard deviation decaying as $1/r^{\alpha}$ for sites at a distance $r \gg b$, where b is a typical bandwidth. It was shown that this model presents an Anderson-like transition at $\alpha = 1$, with all states being localized for $\alpha > 1$ and extended for $\alpha < 1$. The Anderson transition in a 1D chain with random power-law decaying hopping terms and non-random on-site energies was numerically characterized in [27]. Vibrational and one-magnon excitations in one-dimensional systems with power-law decaying long-range couplings have also been shown to depict a localization–delocalization transition [28, 29].

A relevant variation of the Anderson localization is the quantum percolation problem. Due to its simplicity, several

applications of quantum percolation concepts have been used to investigate the transport properties of granular systems and wave propagation in random binary media, as well as in proposals of new nanostructured devices [30–33]. The quantum percolation phenomenon incorporates both classical percolation features and quantum transport properties in disordered systems. In classical percolation, the minimal condition for the transport is the existence of a spanning cluster which appears for bond probabilities above a minimum threshold p_c. The quantum percolation problem is correlated to the properties of transmission and reflection of the wavefunction throughout the irregular borders of the connected cluster. Quantum percolation occurs above p_q, which is usually larger than p_c.

The problem of quantum percolation in 1D disordered systems with long-range hopping terms has been recently addressed [34, 35]. In [34], the authors have considered a bond-diluted model where the links are activated with probability $p(r) = p/r^{1+\sigma}$, where p is the fraction of nearest-neighbor bonds, σ controls the long-range character of the couplings and r is the distance between the two sites to be connected with probability $p(r)$. For this model, a spanning cluster of connected sites rises above a classical percolation threshold p_c. For $\sigma > 1$ there is no spanning cluster for any finite dilution of the first-neighbor bonds. In [35], the particular case of $p = 1$ was reported. Using an exact diagonalization scheme on finite chains, it was computed the spreading of an initially localized wavepacket and the time-dependent participation number, as well as the return probability. The numerical results indicated the existence of extended states below a critical value of the decay exponent σ.

In the present work, we advance in the characterization of the power-law bond-diluted Anderson chain model by studying the quantum percolation transition in the full range of first-neighbor bond probability. Using direct diagonalization of the Hamiltonian matrix on finite chains, we will determine the density of states and nature of the one-particle eigenstates. The density of states will be shown to depict singularities related to specific degenerate localized modes. Using a finite-size scaling analysis based on phenomenological finite-size scaling analysis, we will determine the critical value of the decay exponent σ below which extended modes appear as a function of the first-neighbor bond probability p. We will show that there is a phase on which, although classical percolation is supported by a spanning cluster, all electronic eigenstates are exponentially localized. Finally, the fractal exponent related to the participation number of the critical eigenstates will be reported.

In section 2, we will present our Hamiltonian model, define the main quantities we will use and describe the procedure we will employ to investigate the quantum percolation transition. In section 3, we present our main results concerning the density of states, the participation number, its finite-size scaling, and the phase diagram and fractal exponent of the critical participation function. In section 4 we summarize and draw our main conclusions.

2. Model and formalism

The quantum percolation problem in a bond-diluted chain with non-random long-range hopping amplitudes can be represented by an one-electron tight-binding Hamiltonian with a single orbital per site. In the atomic orbital wavefunction basis, it is expressed as

$$H = \sum_{n=1}^{N} \epsilon_n |n\rangle\langle n| + \sum_{n\neq m}^{N} h(r)|n\rangle\langle m|, \tag{1}$$

where $|n\rangle$ represents the state with the electron localized at site n. In what follows, we will consider closed chains with N sites for which r is the minimal distance between sites n and m. In the present random bond Anderson model, the on-site potentials ϵ_n are site-independent and in equation (1) it is taken to be $\epsilon_n = 0$ without any loss of generality. Long-range disorder is introduced by assuming the hopping amplitudes $h(r)$ to be distributed following a power-law decaying distribution. The probability of occurrence of a bond between sites n and m decays as

$$p(r) = p/r^{1+\sigma} \tag{2}$$

where $h(r) = 1$ with probability $p(r)$ and $h(r) = 0$ with probability $1 - p(r)$. For $\sigma > 1$ this model is expected to have features similar to those presented by models with random short-ranged couplings [34, 35, 37]. For $\sigma < 0$ the bond distribution is not normalizable and an artificial cutoff has to be added. In this regime, a percolation cluster emerges for any finite concentration p [37]. In our study, we are interested in providing the complete phase diagram concerning the quantum percolation transition in the (p, σ) parameter space in the long-ranged regime $0 < \sigma < 1$ on which the bond distribution is normalizable. The main physical quantities will be obtained by the direct diagonalization of the Hamiltonian on finite chains which provides all eigenstates and energy eigenvalues for each disorder realization. The diagonalization is restricted to the largest cluster of connected sites. The participation function plays a central role in the characterization of the spatial extension of the one-electron eigenstates. For a particular disorder configuration ν and eigenstate, the participation function is defined as the inverse of the second moment of the probability density:

$$\xi^{j,\nu} = \frac{1}{\sum_{n=1}^{N} |f_n^{j,\nu}|^4} \tag{3}$$

where $f_n^{j,\nu}$ is the amplitude at site n of the jth eigenstate from the νth disorder realization. ξ diverges proportional to the number of sites (N) for extended states and it is roughly size-independent for exponentially localized ones. According to the finite-size scaling hypothesis, the participation function at the critical point scales as $\xi \propto N^{D_f}$, with $D_f < 1$ being a characteristic fractal dimension of the critical eigenstates. In our numerical computation, we performed an exact diagonalization of the Hamiltonian matrix corresponding to the spanning cluster on chains with sizes ranging from $N = 200$ up to $N = 1600$ sites. We averaged $\xi^{j,\nu}$ using all

eigenstates computed from distinct disorder realizations:

$$\langle \xi(N,p,\sigma)\rangle = \frac{1}{MN}\sum_{\nu=1}^{M}\sum_{j=1}^{N}\xi^{j,\nu}. \quad (4)$$

We have used at least $NM = 1 \times 10^5$ states for each chain size. By fixing the value of the first-neighbor bond concentration, the critical value of the decay exponent σ, below which extended states appear, can be estimated using a phenomenological finite-size scaling analysis.

At the critical point, the participation function scales sub-linearly with the system size $\langle \xi \rangle \propto N^{D_f}$, where D_f is a characteristic fractal dimension. According to the single-parameter scaling hypothesis, in the vicinity of the critical point σ_c, the participation function shall obey the scaling form $\langle \xi \rangle = N^{D_f} g[(\sigma - \sigma_c)N^{1/\nu}]$, where $g(x)$ is a proper scaling function and ν is the correlation length exponent. Such scaling form of critical quantities has been previously explored in a phenomenological finite-size scaling analysis that provides accurate estimates of the critical point and exponents [37, 38]. The procedure is based on the behavior of the following set of auxiliary functions:

$$\Theta(N_1, N_2, p) = \log(\langle \xi(N_2,p)\rangle / \langle \xi(N_1,p)\rangle)/\log(N_2/N_1). \quad (5)$$

According to the finite-size scaling hypothesis, these functions shall intercept at a common point for any pair of sizes (N_1, N_2), with a possible small spread due to corrections to scaling. The crossing signals the critical point. The value of Θ at the critical point corresponds to the fractal dimension D_f. Therefore, the above procedure allows for a direct estimate of the fractal dimension of the critical wavefunctions besides the critical point. This feature brings an advantage with respect to methods based on the relative fluctuations of the participation number [39, 40] whose scale-invariant point does not provide a direct information of the wavefunction fractality. In the present model, one expects that auxiliary Θ functions, when plotted as a function of the power-law exponent σ, shall have a scale-invariant point below $\sigma = 1$ which delimits the effective onset of the long-range character of the couplings [34, 35, 37].

In addition, we computed the normalized density of states (DOS) defined as $\mathrm{DOS}(E) = (1/MN)\sum_{j,\nu}\delta(E - E^{j,\nu})$. For extended states, the level spacing displays small fluctuations due to level repulsion. On the other hand, wavefunctions of localized states have a very small overlap. These states do not interact effectively and, therefore, there is no correlation between them. In this case, the density of states depicts increased fluctuations. We can use this concept to provide some hints about the nature of electronic states of the system under study.

3. Results and discussion

3.1. DOS and degenerate localized states

We start our analysis by computing the density of states for two sets of parameters ($p = 1$, $\sigma = 0.5$) and ($p = 1$, $\sigma = 1$) as shown in figure 1. Note that, in the ($p = 1$, $\sigma = 0.5$) case, the density of states is relatively smooth, signaling the possible presence of extended states. In the other case ($p = 1$, $\sigma = 1$), we observe larger fluctuations of the density of states, a clear signature that localized states are playing a major hole. It is interesting to notice that the density of states shows some singularities, particularly visible in the localized case. Previous studies of percolation in quantum simple cubic networks, with dilution of both links and sites, have also observed the presence of peaks in the density of states [36]. These were shown to be related with resonance energies with wavefunctions localized in regions near the boundary of the percolating cluster. In our model, we can clearly identify two resonance energies at $E = 0$ and -1. The states with energy $E = -1$ correspond to states localized in pairs of sites (a, b) that are connected to the same set of network sites and are directly interconnected. In this case, we can write

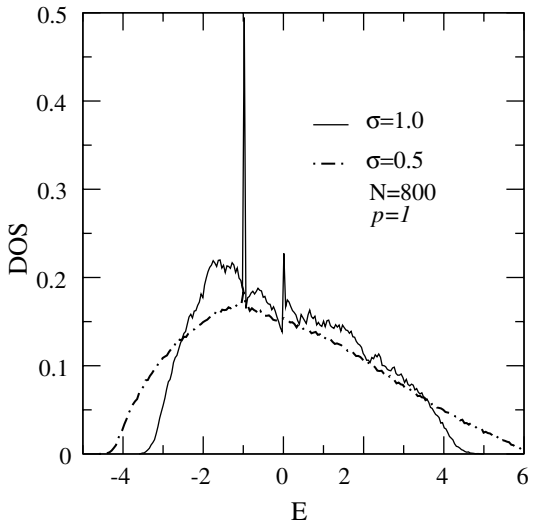

Figure 1. Density of states (DOS) as a function of energy for a chain with $N = 800$, $p = 1$, $\sigma = 0.5$ and 1. For $\sigma = 1$ the density of states displays strong fluctuations, indicating localized states even in the presence of a spanning cluster (geometric percolation). For $\sigma = 0.5$ the DOS is smoother, indicating the presence of extended states. The singularities around $E = -1$ and 0 are related to degenerate localized states.

$$H|a\rangle = |b\rangle + \sum_j |j\rangle, \quad (6)$$

and

$$H|b\rangle = |a\rangle + \sum_j |j\rangle, \quad (7)$$

where the sum is taken over all sites that are connected to the pair (a, b). By subtracting the above equations, it is easily to observe that the antisymmetric state $|\Phi\rangle = (1/\sqrt{2})(|a\rangle - |b\rangle)$ is an eigenstate of the Hamiltonian with eigenvalue $E = -1$. The intensity of the corresponding peak in the density of states is related to the probability of this structure to occur along the chain. The resonance at $E = 0$ corresponds to states localized in pairs of sites (a, b) that, despite being connected to the same set of network sites, they are not directly interconnected. Thus, we have

$$H|a\rangle = \sum_j |j\rangle \quad (8)$$

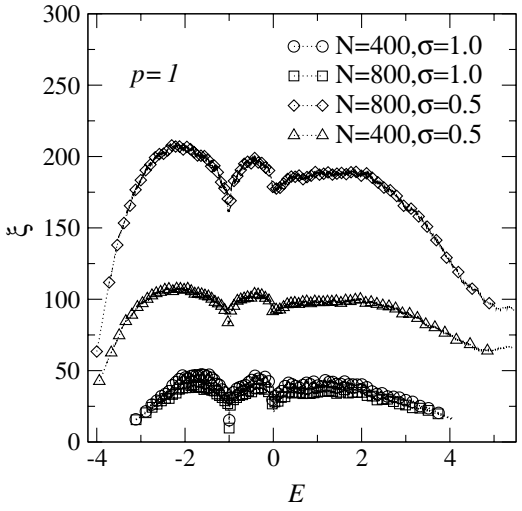

Figure 2. Participation function versus energy for $N = 400$, $N = 800$, $p = 1$, $\sigma = 0.5$ and 1. Data have been averaged over 400 distinct disorder configurations. For $\sigma = 0.5$, the participation function scales linearly with the system size, thus indicating the predominance of extended states. For $\sigma = 1$, the participation function is roughly independent of the system size, signaling the absence of extended states.

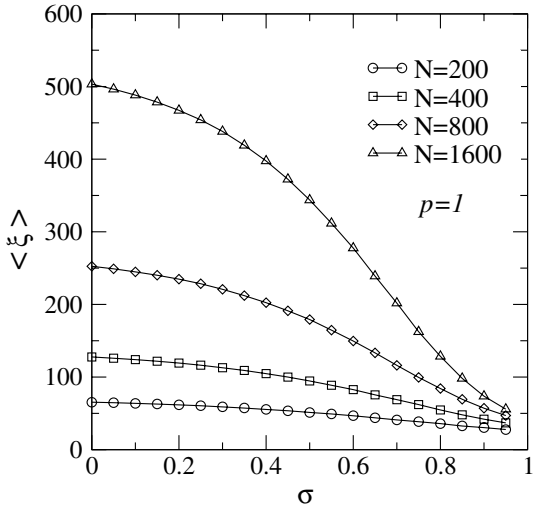

Figure 3. Average participation function for $p = 1$ versus the exponent σ computed using 400 distinct configurations of disorder and different system sizes ($N = 400$ up to 1600). Note the change from the regime of small $\sigma \ll 1$, where the participation function is proportional to the chain size, to the localized regime of large $\sigma \simeq 1$, where $\langle \xi \rangle$ is weakly dependent on N.

and

$$H|b\rangle = \sum_j |j\rangle. \tag{9}$$

In this case, the antisymmetric state $|\Phi\rangle = (1/\sqrt{2})(|a\rangle - |b\rangle)$ is an eigenstate of the Hamiltonian with eigenvalue $E = 0$. The peak in the density of states corresponding to this resonance is smaller than the peak at $E = -1$, since this structure appears along the chain less frequently.

3.2. Quantum percolation transition

In figure 2, we show the energy spectrum of the participation function. These data were obtained through the direct diagonalization of the Hamiltonian for chains with sizes $N = 400$ and 800. Calculations were averaged over 400 distinct disorder realizations. In this figure, we have $p = 1$ for which all first-neighbor pairs are connected. In this case, there is geometric percolation for any value of σ. However, the disorder present in the random coupling of non-first-neighbor pairs can cause the localization of the electronic states. For $\sigma = 1$ the participation function is roughly independent of the chain size for the whole energy band, indicating that all electronic states are localized. For $\sigma = 0.5$, the participation function scales linearly with the system size. It is a clear signature of extended states. Therefore, our results suggest that there is a critical value σ_c at which a quantum percolation transition takes place. The dips at $E = -1$ and 0 reflect the presence of degenerate localized states, as discussed above.

To locate the critical point, we measured the average participation $\langle \xi \rangle$ of the one-particle eigenstates. In figure 3, we show data for the averaged participation function versus the exponent σ for $p = 1$ computed using 400 distinct configurations of disorder and different system sizes ($N = 400$ up to 1600). Note the change from the regime of extended states at small σ, where the participation is proportional to the chain size, to the localized regime where $\langle \xi \rangle$ is roughly size-independent. By using a set of the auxiliary functions $\Theta(N, N', \sigma)$ (see equation (5)), we can precisely locate the critical point $\sigma_c(p)$ as the intersection of curves for different system sizes. Two representative results of this crossing are shown in figure 4 for $p = 0.5$ and 0.75.

The above numerical finite-size scaling method was used to obtain the complete phase diagram of the quantum percolation transition in the (p, σ) parameter space. The results are reported in figure 5 and compared with the phase diagram of the classical percolation counterpart model [37]. The small error bars in the estimated quantum percolation threshold results from the small spread of the crossing point of distinct auxiliary Θ functions. Below the quantum percolation threshold $p_c(\sigma)$ all states are localized while above it extended states emerge. As expected, the quantum percolation threshold (p^{quantum}) exceeds the equivalent classical one ($p^{\text{classical}}$) for all values of σ within the interval [0, 1]. Therefore, there is a finite region of the parameter space at which there is no quantum percolation although a spanning cluster supports classical percolation. In the region of small σ the difference between p^{quantum} and $p^{\text{classical}}$ is small, but it grows as σ grows. We can observe that quantum percolation is absent for $0.78 < \sigma < 1$ even for $p = 1$ where all first neighbors are connected.

3.3. Fractal dimension of the critical states

Before finishing, we also report the fractal dimension D_f at the critical point within the entire range $0 < p < 1$, as shown in figure 6. In the limit $p \to 1$, $D_f < 1$ indicates that the critical eigenstates display a fractal topology, i.e. they do not occupy the entire connected system. In this limit the connected sites

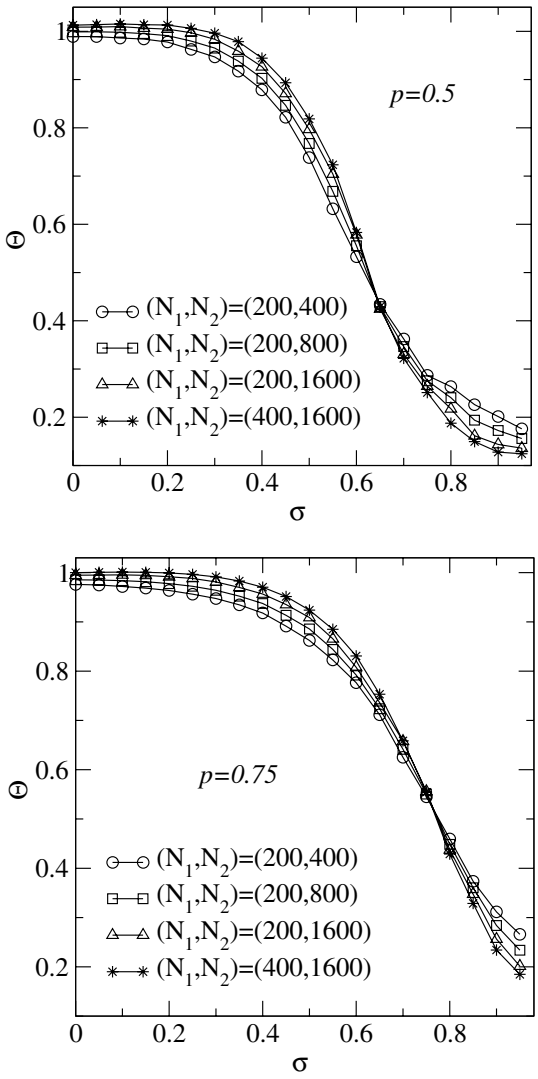

Figure 4. $\Theta(N_1, N_2, \sigma)$ as a function of the decay exponent σ for different pairs of system sizes, $p = 0.5$ and 0.75. Calculations were done using over than 20 000 configurations of disorder. The interception point signal the quantum percolation transition at $\sigma_c(p)$.

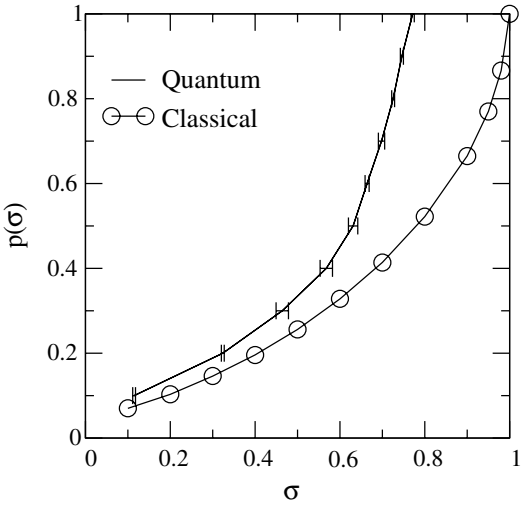

Figure 5. The estimated phase diagram for the long-range quantum percolation model with power-law decaying bond concentrations. Critical points were estimated from direct diagonalization of the bond matrix of the largest cluster and a phenomenological finite-size scaling analysis. The results are compared with the phase diagram of the classical counterpart model [37]. Note that there is a region in which there is classical percolation but no quantum percolation.

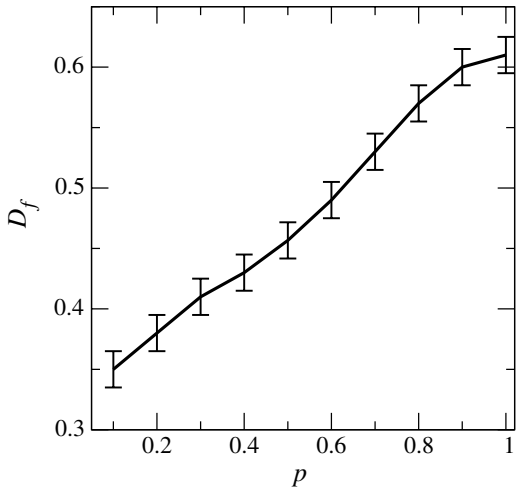

Figure 6. Fractal dimension of the critical wavefunctions as a function of the fraction of first-neighbor couplings p. In the limit of $p \to 1$, $D_f < 1$ indicates that the critical states display a fractal topology. In the other extreme, where $p \to 0$, the fractal dimension of the critical wavefunctions is similar to the fractal dimension of the classical percolating cluster [37].

span the entire lattice. The present finding of $D_f < 1$ in this limit is consistent with the well-known fractal character of the critical wavefunctions in regular lattices. In the opposite limit, $p \to 0$, the fractal dimension of the critical states becomes of the order of the fractal dimension of the percolating cluster $d_f \simeq 0.35$ [37], indicating that the critical states occupy uniformly the spanning cluster. This represents the limit of weak disorder for which the one-particle eigenstates spreads over the entire set of connected sites, with the quantum and classical percolation transition taking place simultaneously as indicated in the reported phase diagram (figure 5).

4. Summary and conclusion

In summary, we studied a one-dimensional tight-binding model with long-ranged hopping amplitudes, where the probability of connection between sites at a distance r is given by $p(r) = p/r^{1+\sigma}$. By using exact diagonalization of the Hamiltonian, we analyzed some features of the density of states and participation function of all eigenstates. The localized or extended nature of the eigenstates was shown to be reflected in the statistical fluctuations of the density of states, as well as in the dependence of the participation function with the system size. Within the density of state analysis, we have shown the existence of singularities at some resonance energies and demonstrated these to originate from degenerate states localized in some local configurations with special symmetries.

Using a phenomenological finite-size scaling analysis, the complete phase diagram in the (p, σ) parameter space was obtained. The critical concentration $p(\sigma)$ in this quantum percolation model was shown to be larger than the geometric percolation critical threshold. Thus, this model presents a phase for which, despite the existence of a percolating cluster, all the electronic states remain localized. Extended states arise in this model for $\sigma < 0.78$. For $p \ll 1$ the fractal dimension of electronic states at the critical point was found to be of the same order of the fractal dimension of the classical percolating cluster. At $p = 1$, the fractal dimension is smaller than the size of the chain, indicating that the critical state does not occupy the percolating cluster uniformly.

It is important to emphasize that the well-known 1D Anderson model with random on-site energies and non-random long-range hopping requires a slower decay of the hopping amplitudes to support extended states ($\sigma < 0.5$) [20–22]. Further, the power-law random band model with random off-diagonal amplitudes with variance decaying as a power law requires $\sigma < 0$ for the emergence of delocalized states [23–26]. Our present model is a clear example that the quantum percolation transition has not always a direct relation with the usual Anderson transition. Further developments would be in order to establish the full set of critical exponents as a function of the decay exponent of the long-ranged couplings.

Acknowledgments

This work was partially supported by CNPq, CAPES and FINEP (Federal Brazilian agencies) and INCT-Nano(Bio)Simes, as well as FAPEAL (Alagoas State Agency).

References

[1] Anderson P W 1958 *Phys. Rev.* **109** 1492
[2] Abrahams E, Anderson P W, Licciardello D C and Ramakrishnan T V 1979 *Phys. Rev. Lett.* **42** 673
[3] Kramer B and MacKinnon A 1993 *Rep. Prog. Phys.* **56** 1469
Ziman T A L 1982 *Phys. Rev. Lett.* **49** 337
For a review see, e.g. Lifshitz I M, Gredeskul S A and Pastur L A 1988 *Introduction to the Theory of Disordered Systems* (New York: Wiley)
[4] Mott N F 1967 *Adv. Phys.* **16** 49
[5] Flores J C 1989 *J. Phys.: Condens. Matter* **1** 8471
[6] Dunlap D H, Wu H L and Phillips P W 1990 *Phys. Rev. Lett.* **65** 88
Wu H-L and Phillips P 1991 *Phys. Rev. Lett.* **66** 1366
[7] Domínguez-Adame F, Maciá E and Sánchez A 1993 *Phys. Rev.* B **48** 6054
[8] de Moura F A B F and Lyra M L 1998 *Phys. Rev. Lett.* **81** 3735
[9] de Moura F A B F, Coutinho-Filho M D, Raposo E P and Lyra M L 2002 *Phys. Rev.* B **66** 014418
[10] de Moura F A B F, Coutinho-Filho M D, Raposo E P and Lyra M L 2003 *Phys. Rev.* B **68** 012202
[11] Izrailev F M and Krokhin A A 1999 *Phys. Rev. Lett.* **82** 4062
Izrailev F M, Krokhin A A and Ulloa S E 2001 *Phys. Rev.* B **63** 41102
[12] Zhang G P and Xiong S-J 2002 *Eur. Phys. J.* B **29** 491
[13] Bellani V, Diez E, Hey R, Toni L, Tarricone L, Parravicini G B, Domínguez-Adame F and Gómez-Alcalá R 1999 *Phys. Rev. Lett.* **82** 2159
[14] Bellani V, Diez E, Parisini A, Tarricone L, Hey R, Parravicini G B and Domínguez-Adame F 2000 *Physica* E **7** 823
[15] Shima H, Nomura T and Nakayama T 2004 *Phys. Rev.* B **70** 075116
[16] Kuhl U, Izrailev F M, Krokhin A and Stöckmann H J 2000 *Appl. Phys. Lett.* **77** 633
[17] de Moura F A B F and Lyra M L 1999 *Physica* A **266** 465
Cheraghchi H, Fazeli S M and Esfarjani K 2005 *Phys. Rev.* B **72** 174207
[18] Schubert G, Weiße A and Fehske H 2005 *Physica* B **359–361** 801
[19] de Brito P E, Rodrigues E S and Nazareno H N 2004 *Phys. Rev.* B **69** 214204
[20] Rodríguez A, Malyshev V A and Domínguez-Adame F 2000 *J. Phys. A: Math. Gen.* **33** L161
[21] Rodríguez A, Malyshev V A, Sierra G, Martín-Delgado M A, Rodríguez-Laguna J and Domínguez-Adame F 2003 *Phys. Rev. Lett.* **90** 27404
[22] Malyshev A V, Malyshev V A and Domínguez-Adame F 2004 *Phys. Rev.* B **70** 172202
[23] Mirlin A D, Fyodorov Y V, Dittes F-M, Quezada J and Seligman T H 1996 *Phys. Rev.* E **54** 3221
[24] Mirlin A D and Evers F 2000 *Phys. Rev.* B **62** 7920
Evers F and Mirlin A D 2000 *Phys. Rev. Lett.* **84** 3690
[25] Mildenberger A, Subramaniam A R, Narayanan R, Evers F, Gruzberg I A and Mirlin A D 2007 *Phys. Rev.* E **75** 094204
[26] Lima R P A, Lyra M L and Cressoni J C 2001 *Physica* A **295** 154
[27] Lima R P A, da Cruz H R, Cressoni J C and Lyra M L 2004 *Phys. Rev.* B **69** 165117
[28] Lima R P A and Lyra M L 2003 *Physica* A **320** 398
[29] Morais P A, Andrade J S Jr, Nascimento E M and Lyra M L 2011 *Phys. Rev.* E **84** 041110
[30] Mookerjee A, Dasgupta I and Saha T 1995 *Int. J. Mod. Phys.* B **9** 2989
[31] Phillips J C 1991 *Phil. Trans. R. Soc.* A **334** 451
[32] Dellacasa V and Feduzi R 1995 *Physica* C **251** 156
[33] Kodama Y and Maekawa T 1999 *Nanotechnology* **10** 217
[34] Lima R P A and Lyra M L 2001 *Physica* A **297** 157
[35] da Silva M P Jr, Albuquerque S S, de Moura F A B F and Lyra M L 2008 *Braz. J. Phys.* **38** 43
[36] Berkovits R and Avishai Y 1996 *Phys. Rev.* B **53** 16125
Schubert G, Weiße A and Fehske H 2005 *Phys. Rev.* B **71** 045126
[37] Albuquerque S S, de Moura F A B F, Lyra M L and Souza A J 2005 *Phys. Rev.* E **72** 016116
[38] Sahimi M 1985 *J. Phys. A: Math. Gen.* **18** 3597
[39] Evers F and Mirlin A D 2000 *Phys. Rev. Lett.* **84** 3690
Evers F and Mirlin A D 2000 *Phys. Rev.* B **62** 7920
[40] Malyshev A V, Malyshev V A and Domínguez-Adame F 2004 *Phys. Rev.* B **70** 172202